Biochimica et Biophysica Acta 1818 (2012) 1378–1385

Contents lists available at SciVerse ScienceDirect

Biochimica et Biophysica Acta

journal homepage: www.elsevier.com/locate/bbamem

The role of sulfatide lipid domains in the membrane pore-forming activity of cobra cardiotoxin

Po-Long Wu [a,c], Chang-Ru Chiu [a], Wei-Ning Huang [b,*], Wen-Guey Wu [a,**]

[a] Department of Life Science, National Tsing Hua University, Hsinchu, Taiwan
[b] Department of Biotechnology, Yuanpei University, Hsinchu, Taiwan
[c] Environment and Biotechnology Department, Refining and Manufacturing Research Institute, CPC Corporation, Chiayi, Taiwan

ARTICLE INFO

Article history:
Received 15 September 2011
Received in revised form 20 January 2012
Accepted 15 February 2012
Available online 23 February 2012

Keywords:
Cardiotoxin
Pore
Lipid domain
Sulfatide

ABSTRACT

Cobra CTX A3, the major cardiotoxin (CTX) from *Naja atra*, is a cytotoxic, basic β-sheet polypeptide that is known to induce a transient membrane leakage of cardiomyocytes through a sulfatide-dependent CTX membrane pore formation and internalization mechanism. The molecular specificity of CTX A3-sulfatide interaction at atomic levels has also been shown by both nuclear magnetic resonance (NMR) and X-ray diffraction techniques to reveal a role of CTX-induced sulfatide conformational changes for CTX A3 binding and dimer formation. In this study, we investigate the role of sulfatide lipid domains in CTX pore formation by various biophysical methods, including fluorescence imaging and atomic force microscopy, and suggest an important role of liquid-disordered (*ld*) and solid-ordered (*so*) phase boundary in lipid domains to facilitate the process. Fluorescence spectroscopic studies on the kinetics of membrane leakage and CTX oligomerization further reveal that, although most CTXs can oligomerize on membranes, only a small fraction of CTXs oligomerizations form leakage pores. We therefore suggest that CTX binding at the boundary between the *so* and *so*/*ld* phase coexistence sulfatide lipid domains could form effective pores to significantly enhance the CTX-induced membrane leakage of sulfatide-containing phosphatidylcholine vesicles. The model is consistent with our earlier observations that CTX may penetrate and lyse the bilayers into small aggregates at a lipid/protein molar ratio of about 20 in the ripple $P_{\beta'}$ phase of phosphatidylcholine bilayers and suggest a novel mechanism for the synergistic action of cobra secretary phospholipase A2 and CTXs.

1. Introduction

Sphingolipids are ubiquitous constituents of all mammalian plasma membranes. A diverse array of pathogens and protein toxins are known to target sphingolipids [1–3]. For example, the ganglioside GM1, globo-triaosylceramide, and globo-tetraosylceramide have been shown to be the receptor for the cholera toxin from *Vibrio cholera* [4], shiga toxin from *Escherichia coli* and the pig edema disease toxin, respectively [5]. Interestingly, in additional to the lipid binding specificity, the formations of sphingolipid domains, or the so-called lipid rafts, have also been suggested to significantly modulate important biological activities [6]. Thus, δ-lysin, a secreted peptide from *Staphylococcus aureus*, preferentially binds to liquid-disordered *(ld)* domains, which concentrates the toxin and leads to dye efflux from lipid vesicles [7]. Melittin, a toxin from bee venom, increases membrane leakage of sphingomyelin containing vesicles because it forms transmembrane pores when the solid-ordered (*so*) and liquid-disordered (*ld*) phase, *i.e.*, *so*/*ld* phase, coexist [8]. The membrane binding affinity of sea anemone-derived equinatoxin II is also strongly enhanced by the presence of sphingomyelin and forms pores only under the liquid-ordered (*lo*)/*ld* coexistence phase [9]. How the existence of sphingolipid domains could modulate biological activities of pore formation toxins in the plasma membrane is of current biophysical interests [10–13].

Cobra cardiotoxins (CTXs) are 60–62 amino acid amphiphilic polypeptides consisting of extended β-sheets with a three-fingered loop folding topology [14]. CTXs are water-soluble proteins and have strong binding affinities on negatively charged membrane [15]. *In vivo*, CTXs cause systolic heart arrest, severe tissue necrosis, and/or blindness [16]. *In vitro*, CTXs cause general cytotoxicity in many cell types such as bacterial cells, human erythrocytes, cancer cells, and cardiomyocytes [17–20]. Although other membrane targets such as glycosaminoglycans or integrins have been shown to bind to distinct type of CTXs and modulate CTX activities [21–25], the lipid binding ability of CTXs, followed by their pore forming activity, is believed to play important roles in the CTX-induced toxicity. As a membrane acting toxin, CTXs induce membrane aggregation, fusion,

* Correspondence to: W.N. Huang, Department of Biotechnology, Yuanpei University, No. 306, Yuanpei Street, Hsinchu 30015, Taiwan. Tel.: +886 03 5381183x8160; fax: +886 03 6102312.
** Correspondence to: W.G. Wu, Department of Life Science, National Tsing Hua University 101, Section 2, Kuang-Fu Road, Hsinchu 30013, Taiwan. Tel.: +886 3 5731040; fax: +886 03 5717237.
E-mail addresses: wnhuang@mail.ypu.edu.tw (W.-N. Huang), wgwu@life.nthu.edu.tw (W.-G. Wu).

0005-2736/$ – see front matter © 2012 Elsevier B.V. All rights reserved.
doi:10.1016/j.bbamem.2012.02.018

and leakage of phospholipid vesicles [26–28] and therefore also named as cytotoxins [14]. However, recent studies on the action of CTX A3 (a major CTX from Taiwan cobra venom) on cardiomyocytes have suggested sulfatide as its specific target. Monoclonal antibodies raised against sulfatide (sulfogalactosylceramide, SGC) are capable of inhibiting the action of CTX A3 to prevent membrane leakage and cell internalization [29,30]. CTX A3 forms pores specifically in sulfatide-containing vesicles with pore sizes and lifetimes in the range of about 30 Å and 10^{-2} s, respectively [31]. The crystal structure of the CTXA3/sulfatide complex reveals an unexpected orientation for the sulfatide fatty chains and sheds light on a possible mechanism of lipid-mediated toxin translocation [32]. Since sulfatides exist in the outer leaflet of most eukaryotic plasma membranes including male germ cells, myelin sheath cells, and epithelial cells [33] and have been classified as a component of lipid rafts [34,35], it is interesting to know whether sulfatide lipid domains are also involved in its pore forming activity.

In this study, we investigate the role of sulfatide lipid domains in CTX pore formation by various biophysical methods, including fluorescence imaging and atomic force microscopy. A phase diagram of sulfatide/1-palmitoyl-2-oleoyl-*sn*-glycerol-3-phosphocholine (POPC) mixture is also presented and correlated with CTX-induced membrane leakage activity. By comparing how phosphatidylserine (PS)- and sulfatides-containing membranes could differentially modulate the oligomerization process of CTXs and their related membrane leakage activity, we demonstrate the existence of sulfatide lipid domains and its important role in regulating CTX pore formation. The results suggest that effective CTX pore formation followed by CTX oligomerization only occurs at the sulfatide lipid domain boundary. Since secretary phospholipase A2 is also ubiquitously present in cobra venom and has been shown recently to restructure membranes in the presence of lipid domains [11], a novel mechanism is proposed to explain the synergistic action between phospholipase A2 and CTXs.

2. Materials and methods

2.1. Materials and purification

All lipids, 1-palmitoyl-2-oleoyl-*sn*-glycerol-3-phosphocholine (POPC), 1-palmitoyl-2-oleoyl-*sn*-glycero-3-phospho-L-serine/sodium salt (POPS), and sulfatides/porcine brain/ammonium salt were obtained commercially from Avanti Polar Lipids (Alabaster, AL). Cholesterol, 6-carboxyfluoresein (CF), rhodamine B isothiocyanate and 1,6-diphenyl-1,3,5-hexatriene (DPH) were purchased from Sigma Aldrich (St. Louis, MO). 1,1′-dioctadecyl-3,3,3′,3′-tetramethylindocarbocyanine perchlorate (DiIC18) was purchased from Invitrogen (U.S.A.). CTX A3 and rhodamine-labeled CTX A3 (Rh-A3) were purified and conjugated as previously described [31]. Briefly, CTX A3 was purified by applying crude venoms (from Snake Education Farm, Tainan, Taiwan) to a SP-Sephadex C-25 ion exchange column chromatograph followed by HPLC on a reverse-phase C-18 column. The purity of all toxins was verified by SDS-PAGE, HPLC and mass spectrometry.

2.2. Membrane vesicle leakage assay and CTX oligomerization measurement

For leakage assays, lipids were dried under nitrogen gas and vacuum and then hydrated with 10 mM Tris (pH 7.4) containing 75 mM NaCl and 50 mM CF. Lipid mixtures were extruded through polycarbonate filters (pore size 0.1 μm) to obtain homogeneous large unilamellar vesicles (LUVs). The residual fluorescence molecules on the outside of the vesicles were removed using a Sepharose CL-4B column with 10 mM Tris (pH 7.4), 150 mM NaCl buffer solution. The CF leakage was calculated using the following expression: leakage = ($Ft - Fi$)/($Ff - Fi$), where Fi is the initial fluorescence before adding proteins, Ft is the fluorescence reading at time t, and Ff is the final fluorescence determined by adding 0.02% Triton X-100 [36]. Fluorescence was excited at 480 nm and emitted at 520 nm.

For evaluation of temperature effect on leakage, the cuvette including vesicle solutions was first incubated at the desired temperature by a circulating water system for 10 min and then the desired amount of CTX A3 was added. The temperatures were monitored directly inside the cuvette with a thermocouple thermometer. Different samples were used for each temperature measuring experiment.

For oligomerization assays, LUVs were prepared with a 10 mM Tris (pH 7.4), 150 mM NaCl buffer solution without going through the procedure with the CL-4B column purification. Varying concentrations of Rh-A3 were added to the vesicle solution (10 μM) and the ability of CTX A3 to oligomerize is monitored by fluorescence resonance energy transfer between identical probes (homo-FRET) by exciting and emitting at 550 nm and 580 nm, respectively.

2.3. Monolayer penetration

Monolayer experiments were done on a Langmuir minitrough (Joyce-Laebl Ltd.) as previously reported [26]. Briefly, surface pressure was determined in a fixed-area, circular Petri dish. The measurements were carried out at the desired temperature and under constant stirring. Lipid mixtures, dissolved in a methanol/chloroform solution, were gently spread onto the air/water interface in the trough and the amounts of lipid mixture were controlled to obtain the desired initial pressure. The subphase solution was prepared in the same manner as the LUVs. The desired amount of CTX A3 (50 nM) was then added for CTX penetration measurement.

2.4. Phase diagram determination of sulfatide/POPC dispersions

The fluorescence anisotropy measurements were carried out on an SLM-4800 spectrofluorometer. The phase diagram for sulfatide/POPC multilamellar vesicles was determined according to Rodrigo F. M. et al. [37]. Briefly, a molar ratio of 0.1% DPH was used as the probe for the fluorescence anisotropy measurements. The DPH containing sample was excited at 360 nm, and the emitted wavelength was recorded at 431 nm. The recorded intensities were used to compute the fluorescence anisotropy $\langle r \rangle$ according to the equation of $\langle r \rangle = (I_{\parallel} - I_{\perp})/(I_{\parallel} + 2I_{\perp})$, where $I_{\parallel}$ and $I_{\perp}$ represent the polarized fluorescence intensity in parallel and perpendicular directions, respectively.

2.5. Fluorescence imaging microscopy

The fluorescence imaging was performed as previously described [38]. Briefly, the experiments were performed in a home-built, wide-field geometry inverted microscope (Olympus IX70; 100× objective). Light from a continuous-wave diode-pumped YAG laser was used to excite at 532 nm and fluorescence images were recorded by an electron multiplying charge-coupled device (EMCCD; Andor Ixon DV-887BI). Andor Solis was used for image acquisition and storage.

2.6. Atomic force microscopy

Supported bilayers were prepared from small unilamellar vesicles (SUV) on mica by the calcium chloride fusion method [39]. Lipid films were dried under vacuum for at least 16 h and then hydrated with buffer containing 10 mM Tris–HCl (pH 7.4) and 150 mM NaCl. After sonication, supported bilayers were prepared by fusion of SUVs (~1 mM) with 10 mM calcium chloride on mica for 1 h. AFM measurements for bilayer samples were carried out on a Picoscan atomic force microscope (Molecular Imaging, MI) in Mac mode with Type II MAClevers (62-014; Molecular Imaging) at 25 °C.

3. Results

3.1. CTX-induced membrane leakage on sulfatides or POPS containing POPC large unilamellar vesicles

We have previously shown by fluorescence spectroscopic measurement on the membrane pore forming activities by comparing the retention ratio between fluorescence probe with different molecular weight such as dextran probe of FD-70 and FD-4 and concluded that the CTX A3-induce pore in sulfatide containing vesicles is ~25–30 Å diameter [31]. The CTX A3 pores in sulfatide containing POPC vesicles are similar to the CTX A3 pores observed in cardiomyocyte membranes. But, it is more stable and smaller than those observed in the less selective PS containing membranes.

Similar conclusion can also be reached based on the kinetic measurement of the CTX A3-induced membrane leakage of 6-CF probe (Fig. 1A and B), showing that CTX A3 is more potent in inducing vesicle leakage in sulfatide containing vesicle. For instance, at 20% leakage of the 6-CF trapped in POPS-containing vesicles, 200 nM CTX A3 was required. But, about one-tenth the concentration of CTX A3 can generate a similar effect on sulfatide-containing vesicles. Under these conditions, the initial rate for CTX A3-induced leakage was ~80%/min and 25%/min for POPS- and sulfatide-containing vesicles, respectively. Thus, the faster initial leakage rate of the POPS containing vesicles, an indication of a larger size of CTX A3 pore, is also observed to exhibit a shorter time required to achieve 50% leakage of the vesicle content (Fig. 1C). The half-time required for the leakage process decreases as the concentration of CTX A3 increases, suggesting that the reaction order of leakage was higher than one.

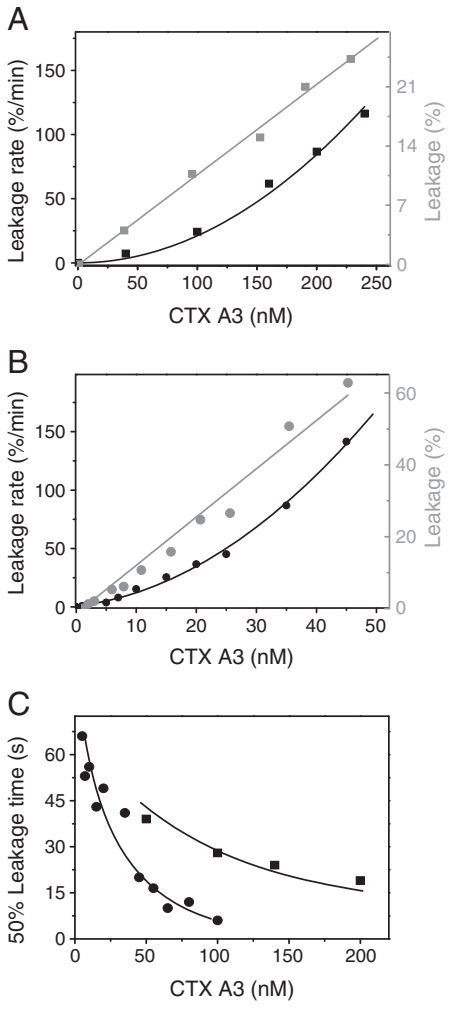

Fig. 1. Fluorescence spectroscopic investigation on the kinetics of membrane pore forming activities as monitored by the CTX A3-induced leakage of 6-CF probe in one to one molar ratio of (A) POPS- or (B) sulfatide-containing POPC membrane vesicles: The initial rate (left y-axis) and total amount (right y-axis) of membrane leakage of 6-CF in LUV (10 μM) were studied at 25 °C and plotted against the designated CTX A3 concentrations. While the initial leakage rates increase as a square of CTX concentration, the total amount of leakage depends linearly on the CTX amount added to the vesicles. (C) At higher CTX concentration, the time required to induce leakage of 50% 6-CF probe from POPS-(▮) or sulfatide-(◆) containing vesicles becomes shorter.

It is noted that, in the studied CTX A3 concentration from nM to sub-μM range, the initial rate of CTX A3-induced vesicle leakage increased as the square of CTX A3 concentration on both POPS and sulfatide containing vesicles. In contrast, the percentage of final vesicular leakage depended only linearly on CTX A3 concentration. Therefore, under the studied experimental condition, the bimolecular interaction of CTX A3 was involved in the process of pore formation and the percentage of leakage was proportional to the number of pores.

3.2. Kinetics of CTX oligomerization as reflected by the kinetics of fluorescence resonance energy transfer of CTX

In order to see how the detected CTX A3 pore formation is related to the oligomerization process of CTX A3 on the studied membrane vesicles, we measure the fluorescence resonance energy transfer between identical probes (homo-FRET) for CTX A3 labeled with rhodamine, *i.e.*, Rh-A3. Fig. 2A and B shows the dose-dependent homo-FRET of Rh-A3 by monitoring its fluorescence intensity decay as a function of time in POPS and sulfatide-containing vesicles, respectively. When 1.25 nM of Rh-A3 was added into the POPS-containing vesicles, the degree of CTX oligomerization can be seen to increase as reflected by the fluorescence intensity decay to indicate an increase of its homo-FRET as a function of time. In consistent with this interpretation, as the concentrations of Rh-A3 increase to 100 nM, the time required for the fluorescence energy decays by 50%, *i.e.*, $t_{1/2}$, for Rh-A3 on POPS-containing vesicles also decreases to ~2 s (Fig. 2C). Apparently, the $t_{1/2}$ required for CTX oligomerization is much shorter than the time required for observing CTX-induced leakage of 50% 6-CF probe, *i.e.*, 30 s at the studied concentration of 100 nM (see Fig. 1C). It suggests that CTX oligomerization detected by the homo-FRET method is not a rate limiting process for the CTX pore formation on POPS containing vesicles.

When similar experiments are performed on sulfatide containing vesicles, we were surprised to find that, while the fluorescence intensities of Rh-A3 also decayed as a function of time, there was no significant concentration dependent effect within the studied concentration range between 1.25 nM and 100 nM (Fig. 2B). The $t_{1/2}$ remains constant (~240 s) throughout the studied concentration range (Fig. 2C) and appeared to be longer than the time required for 50% leakage of sulfatide-containing vesicles, *i.e.* ~70 s or less for CTX concentration lower than 100 nM. Apparently, most of the CTX oligomerization as reflected by the kinetics of homo-FRET is not related to the CTX A3 pore formation to account for the observed membrane leakage process. One of the possible explanations is that effective pore formation occurs much earlier than the CTX oligomerization detected by this homo-FRET method and/or only a small amount of CTX oligomerization could form effective pore in sulfatide containing vesicles. The slow kinetics of Rh-A3 homo-FRET further suggests that, upon adding to the sulfatide containing vesicles, most CTX A3 might bind at a diffusion-limited area such as the gel phase of sulfatide lipid domain.

3.3. CTX A3 binding at sulfatide lipid domains in sulfatide containing POPC vesicles

We determine the CTX A3 binding domain by using fluorescence imaging microscopy on supported lipid bilayers (Fig. 3). Sulfatide-containing vesicles were fused onto glass to form a single supported bilayer and then doped with DiIC18 (green color in Fig. 3A) to allow

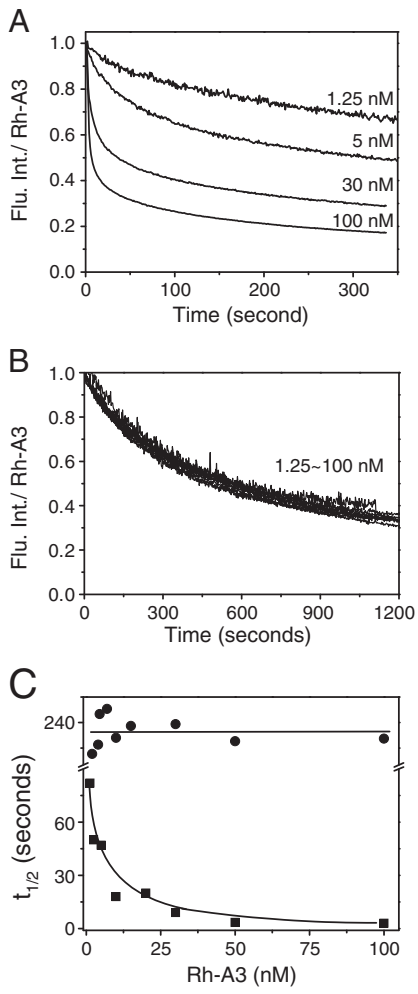

Fig. 2. The kinetics of oligomerization using homo-FRET assays. The fluorescence intensity decay as function of time after different concentrations of Rh-A3 is added to (A) 50% POPS-containing vesicles or (B) 50% sulfatide-containing vesicles. The concentrations of vesicles are 10 μM. The leakage experiments were performed at 25 °C. (C) The time ($t_{1/2}$) required for decay of half of the fluorescence intensity as a function of Rh-A3 concentration in 50% POPS (▮) or 50% sulfatide (◆) containing vesicles.

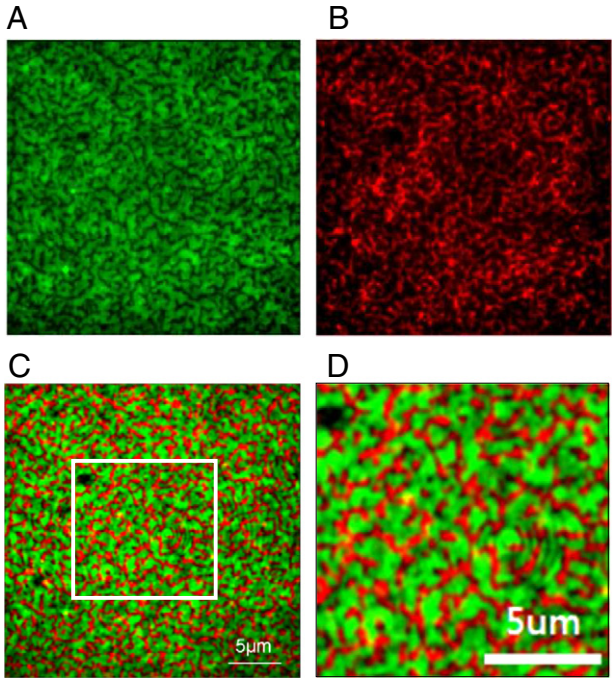

Fig. 3. The fluorescence microscopic images of CTX A3 binding to supported bilayers. (A) The supported bilayers composed of 50% sulfatide membranes (sulfatide/POPC = 1:1 in molar ration) were doped with 1/500 DiIC18 (green), a fluorescence probe identified by FRAP experiments as a tracer for the liquid disordered (*ld*) phase. (B) The fluorescence image of Rhodamine labeled CTX A3 (Rh-A3) bound to supported bilayers. Rh-A3 (50 nM) was added to the water phase of the membrane at 3 min. (C) Superposition of the two images from A and B, showing a complementary pattern of the area for the CTX A3 binding region and lipid *ld* phase region. (D) Enlarged image of panel C, showing the tubule-like structure of sulfatide lipid domain in 50% sulfatide/POPC dispersions.

the visualization of liquid disorder *ld* phase [40]. Interestingly, as shown in Fig. 3C, the red color area responsible for the Rh-A3 binding to sulfatide containing membranes exhibits almost perfect complementary to the green color area responsible for the DiIC18 partitioning *ld* phase (Fig. 3). The mutual exclusive binding of the two fluorescence probes of DiIC18 and Rh-A3 was tested by the statistic analysis of Pearson coefficient [41]. Pearson's coefficient was found to be negative (−0.15), suggesting strongly that most Rh-A3 indeed bind to lipid domains outside the DiIC18 partitioning *ld* phase. Although this observation is consistent with the conjecture that Rh-A3 binds to gel-state sulfatide domain to account for the unexpected large $t_{1/2}$ on sulfatide containing membranes, it is not clear how such a binding could lead to the more effective CTX A3 pore formation responsible for the CTX-induced membrane leakage of the sulfatide containing vesicles.

3.4. Phase diagram of sulfatide containing membranes and its relationship with CTX-induced leakage activity

To correlate the enhanced activity of CTX A3-induced leakage and domain formation on sulfatide containing vesicles, we used DPH molecules as an anisotropy probe for steady-state fluorescence to determine the phase diagram of sulfatide containing POPC dispersions. Fig. 4A shows the representative anisotropy values of the DPH molecule, $\langle r \rangle_{DPH}$, as a function of temperature on sulfatide/POPC mixtures with the designated lipid compositions. Pure (100%) POPC dispersions exhibit $\langle r \rangle_{DPH}$ values below 0.14, suggesting the existence of a *ld* phase for 100% POPC within the studied temperature range from 10 °C to 60 °C. This is consistent with the notion that the Tm of POPC is lower than 0 °C. In contrast, sulfatide dispersions exhibit $\langle r \rangle_{DPH}$ values higher than 0.28 within the temperature range from 10 °C to 40 °C, suggesting the existence of *so* phase in the studied temperature range. The Tm of sulfatides can then be conveniently determined by using the midpoint of the anisotropy transition, occurring at ~45 °C for this particular sulfatide sample. It should be noted that the studied sulfatides were purified from porcine brain and contain both hydroxylated and nonhydroxylated fatty acids with diverse fatty acid chain lengths. Similar results have been reported previously by DSC and anisotropy methods [42].

The $\langle r \rangle_{DPH}$ profiles of the 50% sulfatide sample showed a lower Tm with a broader interval of phase boundary as compared with 100% sulfatide (Fig. 4A and B). As we will show later, temperature dependent studies on the CTX A3-induced leakage of 50% sulfatide containing vesicles could be correlated with the lipid phase separation as detected by this fluorescence anisotropy method (Fig. 4B). Neither pure *ld* phase nor pure *so* phase can provide suitable environment for the CTX A3-induced pore formation process. This is consistent with the previous observation that melittins cause the surface of vesicles to become blurred and also induce dynamic pore formation at the gel-to-liquid crystalline phase transition temperatures [8].

Finally, the efficiency of CTX-induced leakage was also studied as a function of sulfatide concentration in POPC vesicles at 25 °C (Fig. 4C). The CTX-induced leakage becomes most effective when 40% to 50%

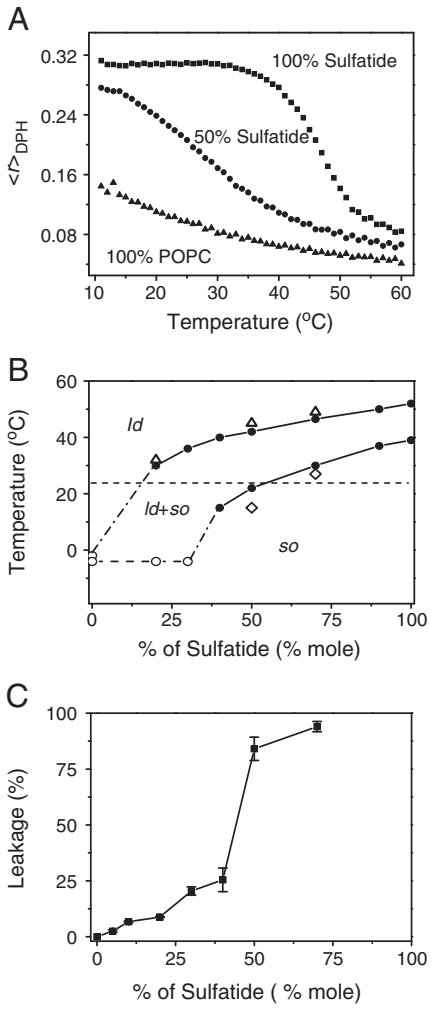

Fig. 4. Sulfatide/POPC phase diagram and its correlation with CTX A3-induced leakage activity. (A) steady-state fluorescence anisotropy of DPH ($\langle r \rangle_{DPH}$) as a function of temperature for MLVs composed of 100% sulfatide, 50% sulfatide and 100% POPC, respectively. (B) Phase diagram of sulfatide/POPC dispersion. The Tm boundaries determined in this study were showed as close circles symbol (●). The point for pure POPC is from Curatolo et al. [54] and hypothetical points were shown in open circles symbols (○). The dotted line is the hypothetical boundary. The leakage activities for the maximum (◇) and transition point of initial leakage (△) are indicated at different percentage of sulfatide-containing LUV and measured as in Fig. 4A. (C) CTX A3-induced leakage of 6-CF probe trapped inside vesicles with the designated percentage of sulfatide-containing vesicles at 25 °C. The phase boundary can be depicted by the horizontal dotted line at the specified sulfatide concentration in POPC dispersions.

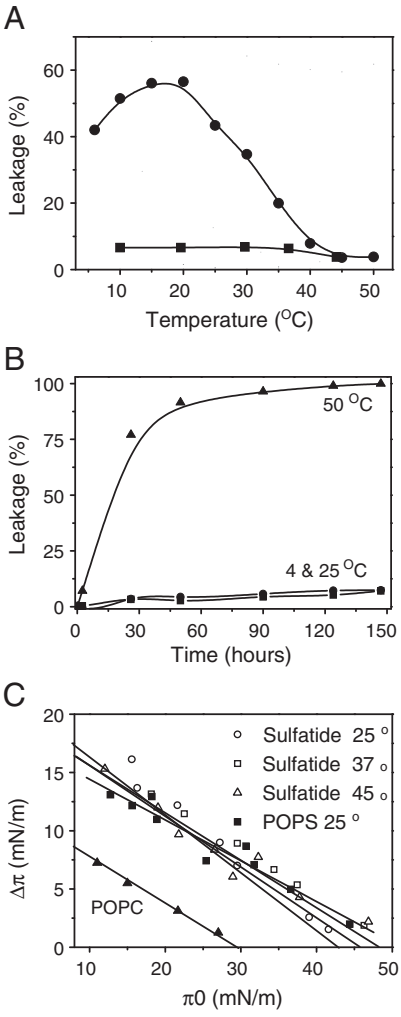

Fig. 5. (A) Temperature dependent CTX A3-induced leakage of the CF probe trapped inside vesicles of 50% POPS (▥) or 50% sulfatide (●) containing vesicles. The concentrations of vesicles and CTX A3 used here are 10 μM and 0.1 μM, respectively. (B) Spontaneous leakages of 6-CF probe were also monitored for 150 h at designated temperature for 50% sulfatide containing POPC vesicles. (C) CTX A3 binding-induced pressure increases of lipid monolayer as a function of the initial pressure in 50% sulfatide or 50% POPS containing POPC monolayer at the indicated temperature.

sulfatide are present in the POPC vesicles while an initial leakage activity could already be observed with the presence of ~10% sulfatide. This corresponds nicely with the phase boundary between *ld*/*so* and *so* phase at the studied temperature of 25 °C (see dashed line in Fig. 4B). These results support our hypothesis that the maximum leakage activities lie close to the boundary of the phase diagram.

3.5. Temperature dependent CTX-induced leakage of sulfatide containing vesicles

With the availability of phase diagram for sulfatide/POPC mixtures, it is interesting to see whether the effect of temperature on the change of lipid phase and thus its related lipid domain could exhibit similar effect on CTX pore forming activity. As shown in Fig. 5A, CTX-induced leakage of sulfatide containing POPC vesicles gradually increased when temperatures decreased from 40 °C with maximum leakage activity occurred at ~17 °C. No such temperature dependent behavior can be detected for POPS containing POPC vesicles. Since other CTX analogs also exhibit similar temperature dependent leakage profiles as CTX A3 (data not shown), we conclude that, in addition to the lipid binding specificity of CTXs, lipid phase domain also play an important role in promoting CTX pore formation. It should be emphasized that the CTX-induced membrane leakage does not depend on the temperature effect on the intrinsic stability of vesicles. At room temperature of 25 °C, there is no significant leakage of the vesicle content up to 6 days. In contrast, the vesicles become unstable at 50 °C as evidenced by the spontaneous leakage of 50% sulfatide containing POPC vesicles (Fig. 5B).

We have previously shown by a combined monolayer, FTIR and computer simulation approach that the electrostatic interaction between anionic lipid and cationic CTXs plays a role in modulating the penetration depth of CTX molecules on the initial peripheral binding mode and reveals a pathway leading to the formation of an inserted mode in negatively charged membrane bilayers [26]. It is therefore possible that a temperature dependent penetration depth of CTX on sulfatide containing membranes could also explain, at least partially, on the temperature dependence of the CTX-induced membrane leakage as observed in Fig. 5A. In order to investigate such a possibility, we applied monolayer experiment on the binding of CTX A3 on sulfatide monolayer as a function of temperature (Fig. 5C). When the

initial surface pressure is at 30 mN/m, an equivalent surface pressure relevant to the biological membrane packing density, CTX A3 indeed can insert into the negatively charged monolayer and create an 8 mN/m increase in surface pressure (Fig. 5C). As we demonstrated previously, CTX A3 did not cause any pressure changes for the 100% POPC monolayer at 30 mN/m initial pressure. This is consistent with the observation that CTX A3 is not unable to form pores on POPC vesicles [31]. However, there is no significant difference for the experiments performed on sulfatide monolayer at three different temperatures of 25 °C, 37 °C and 45 °C. In fact, similar surface expansion can also be observed for the binding of CTX A3 on POPS monolayer at 25 °C (Fig. 5C). These results indicate that the enhanced penetration depth of CTX binding to the negatively charged membranes could not explain the observed temperature-dependence of CTX-induced leakage of sulfatide containing membranes. Sulfatide lipid domains by itself indeed play an important role in modulating CTX A3 pore formation in sulfatide containing POPC membranes.

3.6. Atomic force microscopic investigation on the sulfatide lipid domains

We have so far established that the phase boundary in the sulfatide lipid domain of sulfatide/POPC dispersions plays a role in further modulating CTX pore formation, in addition to the molecular interaction observed previously between CTX A3 and sulfatide molecule. In order to explore more on the possible role of sulfatide lipid domains in promoting CTX A3 pore formation, we used AFM to image the supported sulfatide/POPC bilayer in the presence and absence of cholesterol. Cholesterol has been shown to play an important role in modulating sphingolipid domains in model membranes and is suggested to be rich in biological lipid rafts [43]. As visualized by AFM, the POPS/POPC bilayers appear to be uniformly flat in the liquid phase with only occasional small dots of debris on the surface (panel a in Fig. 6A). This is because the Tm of POPC (−2 °C) and POPS (14 °C) is lower than room temperature. In contrast, POPC membrane bilayers containing 40% (panel b) and 50% sulfatide (panel c) clearly showed a phase separation with quantitative difference in the height of distinct lipid domain. The sulfatide lipid domains for 40% sulfatide/POPC sample exhibit a circular shape with a domain size to be ~50–400 nm in width. It is about 15 Å higher than the surrounding phase as expected from the longer hydrocarbon chain of sulfatide molecules.

More interestingly, as demonstrated in fluorescence imaging microscopic study of sulfatide containing POPC membranes (Fig. 3D), the domain morphology of 50% sulfatide/POPC membranes exhibits a more elongated network domain with ~200–400 nm in width (see panel c in Fig. 6A). There are significant differences in morphologies between 40% and 50% sulfatide containing samples despite of their similarity in the height difference of lipid domains (see panels b and c in Fig. 6A). The relative areas covered by the sulfatide domains were estimated to account for ~50% of the total area from the 50% sulfatide sample. In contrast, the area accountable for the sulfatide domains with higher membrane surface is much less than it is expected from the 40% sulfatide sample. It suggests that there must be significant miscibility of sulfatide in the fluid POPC phase for 40% sulfatide/POPC dispersions. It explains, at partially, the sharp increase in CTX-induced membrane leakage from 40% to 50% sulfatide containing POPC vesicles.

Finally, as shown in panel d of Fig. 6A, the introduction of 25% cholesterol into 50% sulfatide/POPC membrane significantly change both shape and height of the sulfatide lipid domain. Since the presence of cholesterol also significantly inhibit CTX-induced membrane leakage by ~6-folds (compare column c with column d in Fig. 6B), we conclude that sulfatide lipid domains can significantly modulate the pore forming activity of sulfatide binding CTX A3 on sulfatide containing phosphatidylcholine membranes.

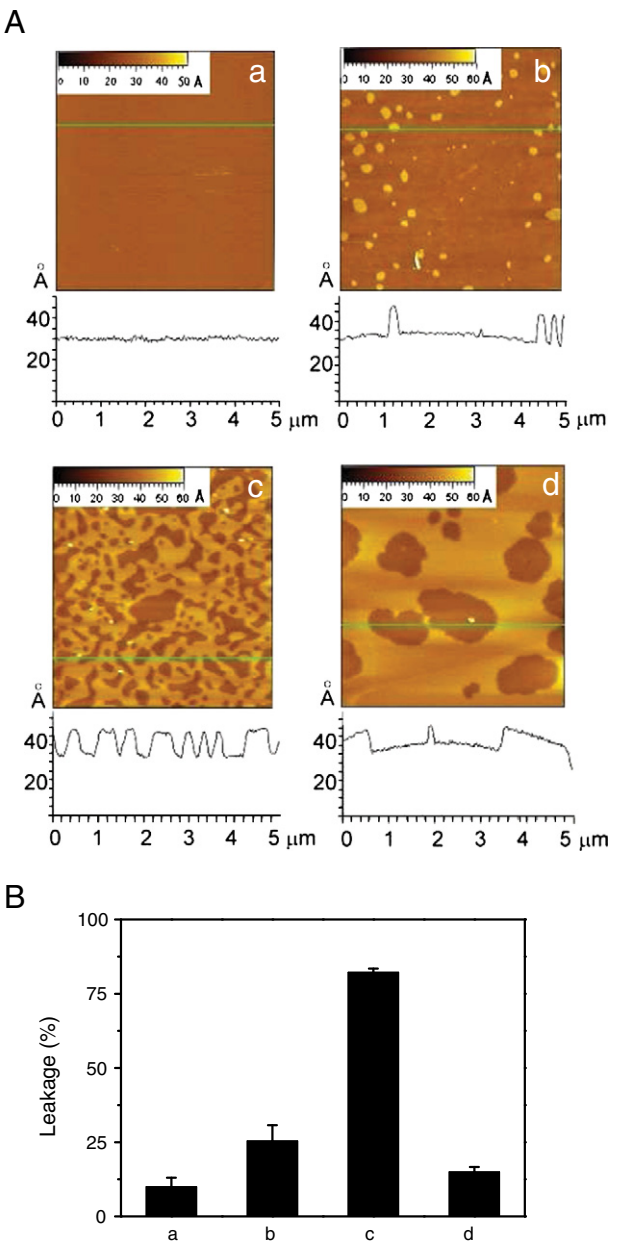

Fig. 6. (A) AFM images of (a) 50% POPS/POPC (b) 40% sulfatide/POPC (c) 50% sulfatide/POPC, and (d) 50% sulfatide/25%POPC/25% cholesterol supported bilayers. The image size is 5 μm^2 and the z-scale is 50 nm. For each image, a section analysis along the horizontal line in the image is shown below the image. (B) Correlation of CTX A3-induced leakage of 6-CF containing vesicles with the phase boundary of sulfatide lipid domains.

4. Discussion

Biological activities of membrane-related processes such as the pore formation of toxins [44], the open and close of ion channels [45], the membrane curvature generation [46–48] and receptor-mediated cell signaling [49] have now been established to involve both hydrophobic and electrostatic interactions between proteins and lipids. Interestingly, the physical interactions underlying these membranes processes often require multi-valency bindings of proteins to membrane lipid domains through a protein-clustering and/or lipid-mediated mechanism [50]. In this study, several spectroscopic and imaging techniques were used to show that effective pore formation of CTX A3, although require a pre-formed sulfatide lipid domain for its high specificity and high affinity binding, could only occur in sulfatide containing POPC dispersions when there exist *so* and *so*/*ld* coexistence

phase of sulfatide lipid domains. Protein binding and oligomerizations on the bilayer surface, as reflected by the kinetics of CTX A3 homo-FRET measurement, are not the rate-limiting process. Most of the CTX A3 molecules are bound on sulfatide-containing *so* domain (Fig. 3) and can only slowly oligomerize due to the slow diffusion of *so* domain. Based on our previous studies, about 8 molecules of CTX A3 can form a pore and induced all-or-none leakage on vesicles [51]. A 100 nm diameter LUV is composed of about 10^5 lipids and 200 CTX A3 molecules are needed for 20% leakage of sulfatide-containing vesicles. This implies that the oligomerizations of most CTX A3 molecules on membrane surface are not effective to form pore. Since the pore forming activity appears to correlate well with the presence of phase boundary of sulfatide lipid domains (Fig. 6), we hypothesize that the exposure of the hydrophobic region in the mismatch boundary sites between distinct lipid phase domain may play an important role to facilitate the penetration of CTX A3 into lipid bilayers to form correct membrane oligomerization and pores.

Three lines of evidence are consistent with the hypothesis. First, by the combined ^{31}P and ^{2}H NMR investigation, in conjunction with DPH fluorescence anisotropy and DSC studies, on the interaction of CTX A3 with zwitterionic dipalmitoyl PC (DPPC) dispersion, we showed that CTX A3 may penetrate and lyse the DPPC bilayers into small aggregates at a lipid/protein molar ratio of ~20 in the ripple $P\beta'$ phase [52]. This suggests that CTX A3 may undergo a re-distribution between penetration and peripheral binding states depending on the presence of distinct lipid phase coexistence. Second, by using the single molecule fluorescence imaging method, we have shown that amphiphilic proteins such as cobra phospholipase A2 may preferentially bind to the packing defect regions of lipid bilayers to facilitate its enzymatic action on the PC molecules. The phase boundary of distinct lipid phase domains, such as the sulfatide lipid domains in sulfatide/POPC dispersions, allows the exposure of the mismatched hydrophobic region and therefore may serve as a packing defect region to facilitate the binding and penetration of amphiphilic CTX A3 molecules. Finally, as we demonstrated in this work, the CTX A3-induced vesicle leakage of sulfatide/POPC dispersions correlates well with the phase boundary of distinct lipid domains.

Many evidences suggest the existence of bilayer packing defect in biological membrane surfaces due to the hydrophobic mismatch of membrane proteins with lipid bilayers and also between distinct lipid domains. Cholesterol in eukaryotic cell membranes has been proposed to play a role to modulate bilayer thickness and its related biological functions. Specifically, variation of cholesterol concentration in the glycosphingolipid raft domain has been shown to either positively or negatively regulate biological activities of membrane proteins. Herein, we showed that the introduction of cholesterol into the sulfatide lipid domains inhibits CTX A3-induced membrane leakage of sulfatide/POPC dispersions (Fig. 6). This observation is consistent with the fact that depriving cholesterol molecules from the plasma membrane of cardiomyocytes could also enhance CTX A3-induced membrane leakage and CTX A3 internalization.

Phospholipase A2 and CTXs are the two major components of cobra venoms and have been suggested to act synergistically for the respective cytotoxicity on many cells. Interestingly, the presence of lipid domains has been shown recently to induce specificity in the hydrolytic activity of phospholipase A2, resulting in marked differences in the physical properties of the membrane end-product [11]. Thus, the involvement of lipid domains in both the enzymatic activity of phospholipase A2 and CTX A3-induced membrane leakage leads to a new possibility that the synergistic action between cobra phospholipase A2 and CTXs may also be modulated by the presence of lipid domains.

It should be pointed out that other lipid components may also be involved in the cytotoxicity of CTXs. For instance, it was reported recently that the leakage ability in PS-containing membranes induced by CTX from *Naja kaouthia* was much more pronounced than those measured for the anionic lipid of sulfatide [53]. Since there are more than seven CTX homologues in Taiwan cobra venom, understanding the combinatorial action of CTX homologues against a distinct type of lipid domains may be needed to fully appreciate the action mechanism of cobra venoms against different cell types. Considering the diverse types of molecules in the plasma membranes and extracellular matrix have now been shown to be a potential target of CTX action [20], future investigation to understand how snake venom works on different cell types may help to establish methods for the understanding of the biological functions in the newly established proteomic world.

Acknowledgements

We thank Linda Johnston for access to atomic force microscopy facilities (NRC, Canada). We also thank Dr. Da-Shin Wang for reading the manuscript and editorial suggestions. This work was supported by a grant from the NSC.

References

[1] S. Manes, G. del Real, A.C. Martinez, Pathogens: raft hijackers, Nat. Rev. Immunol. 3 (2003) 557–568.
[2] A. Singh, M. Del Poeta, Lipid signalling in pathogenic fungi, Cell. Microbiol. 13 (2011) 177–185.
[3] L. Abrami, M. Fivaz, F.G. van der Goot, Adventures of a pore-forming toxin at the target cell surface, Trends Microbiol. 8 (2000) 168–172.
[4] S.V. Heyningen, Cholera toxin: interaction of subunits with ganglioside GM1, Science 183 (1974) 656–657.
[5] S. DeGrandis, H. Law, J. Brunton, C. Gyles, C.A. Lingwood, Globotetraosylceramide is recognized by the pig edema disease toxin, J. Biol. Chem. 264 (1989) 12520–12525.
[6] D. Lingwood, K. Simons, Lipid rafts as a membrane-organizing principle, Science 327 (2010) 46–50.
[7] A. Pokorny, P.F. Almeida, Permeabilization of raft-containing lipid vesicles by delta-lysin: a mechanism for cell sensitivity to cytotoxic peptides, Biochemistry 44 (2005) 9538–9544.
[8] M.J. Gomara, S. Nir, J.L. Nieva, Effects of sphingomyelin on melittin pore formation, Biochim. Biophys. Acta 1612 (2003) 83–89.
[9] P. Schon, A.J. Garcia-Saez, P. Malovrh, K. Bacia, G. Anderluh, P. Schwille, Equinatoxin II permeabilizing activity depends on the presence of sphingomyelin and lipid phase coexistence, Biophys. J. 95 (2008) 691–698.
[10] M. Milescu, F. Bosmans, S. Lee, A.A. Alabi, J.I. Kim, K.J. Swartz, Interactions between lipids and voltage sensor paddles detected with tarantula toxins, Nat. Struct. Mol. Biol. 16 (2009) 1080–1085.
[11] C. Leidy, J. Ocampo, L. Duelund, O.G. Mouritsen, K. Jorgensen, G.H. Peters, Membrane restructuring by phospholipase A2 is regulated by the presence of lipid domains, Biophys. J. 101 (2011) 90–99.
[12] H. Lee, J.A. Rotolo, J. Mesicek, T. Penate-Medina, A. Rimner, W.C. Liao, X. Yin, G. Ragupathi, D. Ehleiter, E. Gulbins, D. Zhai, J.C. Reed, A. Haimovitz-Friedman, Z. Fuks, R. Kolesnick, Mitochondrial ceramide-rich macrodomains functionalize Bax upon irradiation, PLoS One 6 (2011) e19783.
[13] M. Kulma, M. Herec, W. Grudzinski, G. Anderluh, W.I. Gruszecki, K. Kwiatkowska, A. Sobota, Sphingomyelin-rich domains are sites of lysenin oligomerization: implications for raft studies, Biochim. Biophys. Acta 1798 (2010) 471–481.
[14] T.S. Chen, F.Y. Chung, S.C. Tjong, K.S. Goh, W.N. Huang, K.Y. Chien, P.L. Wu, H.C. Lin, C.J. Chen, W.G. Wu, Structural difference between group I and group II cobra cardiotoxins: X-ray, NMR, and CD analysis of the effect of cis-proline conformation on three-fingered toxins, Biochemistry 44 (2005) 7414–7426.
[15] J. Dufourcq, J.F. Faucon, Specific binding of a cardiotoxin from *Naja mossambica mossambica* to charged phospholipids detected by intrinsic fluorescence, Biochemistry 17 (1978) 1170–1176.
[16] A.L. Harvey, Snake Toxins, 1991, pp. 259–298.
[17] N. Zusman, T.M. Miklas, T. Graves, G.E. Dambach, R.A. Hudson, On the interaction of cobra venom protein cardiotoxins with erythrocytes, Biochem. Biophys. Res. Commun. 124 (1984) 629–636.
[18] A. Zaheer, B.M. Braganca, Comparative study of three basic polypeptides from snake venoms in relation to their effects on the cell membrane of normal and tumor cells, Cancer Biochem. Biophys. 5 (1980) 41–46.
[19] W.F. Tzeng, Y.H. Chen, Suppression of snake-venom cardiotoxin-induced cardiomyocyte degeneration by blockage of Ca2+ influx or inhibition of non-lysosomal proteinases, Biochem. J. 256 (1988) 89–95.
[20] L.W. Chen, P.H. Kao, Y.S. Fu, S.R. Lin, L.S. Chang, Membrane-damaging activity of Taiwan cobra cardiotoxin 3 is responsible for its bactericidal activity, Toxicon 58 (2011) 46–53.
[21] P.L. Wu, S.C. Lee, C.C. Chuang, S. Mori, N. Akakura, W.G. Wu, Y. Takada, Non-cytotoxic cobra cardiotoxin A5 binds to alpha(v)beta3 integrin and inhibits bone resorption. Identification of cardiotoxins as non-RGD integrin-binding proteins of the Ly-6 family, J. Biol. Chem. 281 (2006) 7937–7945.

[22] S.C. Tjong, T.S. Chen, W.N. Huang, W.G. Wu, Structures of heparin-derived tetrasaccharide bound to cobra cardiotoxins: heparin binding at a single protein site with diverse side chain interactions, Biochemistry 46 (2007) 9941–9952.
[23] S.C. Lee, H.H. Guan, C.H. Wang, W.N. Huang, S.C. Tjong, C.J. Chen, W.G. Wu, Structural basis of citrate-dependent and heparan sulfate-mediated cell surface retention of cobra cardiotoxin A3, J. Biol. Chem. 280 (2005) 9567–9577.
[24] S.C. Sue, K.Y. Chien, W.N. Huang, J.K. Abraham, K.M. Chen, W.G. Wu, Heparin binding stabilizes the membrane-bound form of cobra cardiotoxin, J. Biol. Chem. 277 (2002) 2666–2673.
[25] W.G. Wu, S.C. Tjong, P.L. Wu, J.H. Kuo, K. Wu, Role of heparan sulfates and glycosphingolipids in the pore formation of basic polypeptides of cobra cardiotoxin, Proteins: Membrane Binding and Pore Formation, in: G. Anderluh, et al., (Eds.), Landes Biosciences, Austin Chapter 12, 2010, pp. 143–148.
[26] W.N. Huang, S.C. Sue, D.S. Wang, P.L. Wu, W.G. Wu, Peripheral binding mode and penetration depth of cobra cardiotoxin on phospholipid membranes as studied by a combined FTIR and computer simulation approach, Biochemistry 42 (2003) 7457–7466.
[27] K.Y. Chien, W.N. Huang, J.H. Jean, W.G. Wu, Fusion of sphingomyelin vesicles induced by proteins from Taiwan cobra (*Naja naja atra*) venom. Interactions of zwitterionic phospholipids with cardiotoxin analogues, J. Biol. Chem. 266 (1991) 3252–3259.
[28] K.Y. Chien, C.M. Chiang, Y.C. Hseu, A.A. Vyas, G.S. Rule, W. Wu, Two distinct types of cardiotoxin as revealed by the structure and activity relationship of their interaction with zwitterionic phospholipid dispersions, J. Biol. Chem. 269 (1994) 14473–14483.
[29] C.H. Wang, R. Monette, S.C. Lee, P. Morley, W.G. Wu, Cobra cardiotoxin-induced cell death in fetal rat cardiomyocytes and cortical neurons: different pathway but similar cell surface target, Toxicon 46 (2005) 430–440.
[30] C.H. Wang, W.G. Wu, Amphiphilic beta-sheet cobra cardiotoxin targets mitochondria and disrupts its network, FEBS Lett. 579 (2005) 3169–3174.
[31] S.C. Tjong, P.L. Wu, C.M. Wang, W.N. Huang, N.L. Ho, W.G. Wu, Role of glycosphingolipid conformational change in membrane pore forming activity of cobra cardiotoxin, Biochemistry 46 (2007) 12111–12123.
[32] C.H. Wang, J.H. Liu, S.C. Lee, C.D. Hsiao, W.G. Wu, Glycosphingolipid-facilitated membrane insertion and internalization of cobra cardiotoxin. The sulfatide.cardiotoxin complex structure in a membrane-like environment suggests a lipid-dependent cell-penetrating mechanism for membrane binding polypeptides, J. Biol. Chem. 281 (2006) 656–667.
[33] D. Lingwood, G. Harauz, J.S. Ballantyne, Regulation of fish gill Na(+)-K(+)-ATPase by selective sulfatide-enriched raft partitioning during seawater adaptation, J. Biol. Chem. 280 (2005) 36545–36550.
[34] D.A. Brown, J.K. Rose, Sorting of GPI-anchored proteins to glycolipid-enriched membrane subdomains during transport to the apical cell surface, Cell 68 (1992) 533–544.
[35] K. Ohta, C. Sato, T. Matsuda, M. Toriyama, W.J. Lennarz, K. Kitajima, Isolation and characterization of low density detergent-insoluble membrane (LD-DIM) fraction from sea urchin sperm, Biochem. Biophys. Res. Commun. 258 (1999) 616–623.
[36] C. Kayalar, N. Duzgunes, Membrane action of colicin E1: detection by the release of carboxyfluorescein and calcein from liposomes, Biochim. Biophys. Acta 860 (1986) 51–56.
[37] R.F. de Almeida, A. Fedorov, M. Prieto, Sphingomyelin/phosphatidylcholine/cholesterol phase diagram: boundaries and composition of lipid rafts, Biophys. J. 85 (2003) 2406–2416.
[38] C.R. Chiu, W.N. Huang, W.G. Wu, T.S. Yang, Fluorescence single-molecule study of cobra phospholipase A2 action on a supported gel-phase lipid bilayer, Chemphyschem 10 (2009) 549–558.
[39] Ira, L.J. Johnston, Sphingomyelinase generation of ceramide promotes clustering of nanoscale domains in supported bilayer membranes, Biochim. Biophys. Acta 1778 (2008) 185–197.
[40] N. Kahya, D. Scherfeld, K. Bacia, B. Poolman, P. Schwille, Probing lipid mobility of raft-exhibiting model membranes by fluorescence correlation spectroscopy, J. Biol. Chem. 278 (2003) 28109–28115.
[41] S. Bolte, F.P. Cordelieres, A guided tour into subcellular colocalization analysis in light microscopy, J. Microsc. 224 (2006) 213–232.
[42] K. Saxena, R.I. Duclos Jr., P.K. Sripada, G.G. Shipley, Unusual hydration properties of C16:0 sulfatide bilayer membranes, Biophys. J. 79 (2000) 385–393.
[43] K. Mitra, I. Ubarretxena-Belandia, T. Taguchi, G. Warren, D.M. Engelman, Modulation of the bilayer thickness of exocytic pathway membranes by membrane proteins rather than cholesterol, Proc. Natl. Acad. Sci. U. S. A. 101 (2004) 4083–4088.
[44] K. Yamashita, Y. Kawai, Y. Tanaka, N. Hirano, J. Kaneko, N. Tomita, M. Ohta, Y. Kamio, M. Yao, I. Tanaka, Crystal structure of the octameric pore of staphylococcal gamma-hemolysin reveals the beta-barrel pore formation mechanism by two components, Proc. Natl. Acad. Sci. U. S. A. 108 (2011) 17314–17319.
[45] H.L Wang, X. Cheng, S.M. Sine, Intra-membrane proton binding site linked to activation of a bacterial pentameric ion channel, J. Biol. Chem. 287 (2012) 6482–6489.
[46] J. Zimmerberg, S. McLaughlin, Membrane curvature: how BAR domains bend bilayers, Curr. Biol. 14 (2004) R250–R252.
[47] S. Suetsugu, K. Toyooka, Y. Senju, Subcellular membrane curvature mediated by the BAR domain superfamily proteins, Semin. Cell Dev. Biol. 21 (2010) 340–349.
[48] J.L. Gallop, C.C. Jao, H.M. Kent, P.J. Butler, P.R. Evans, R. Langen, H.T. McMahon, Mechanism of endophilin N-BAR domain-mediated membrane curvature, EMBO J. 25 (2006) 2898–2910.
[49] B. Antonny, Mechanisms of membrane curvature sensing, Annu. Rev. Biochem. 80 (2011) 101–123.
[50] M.B. Jensen, V.K. Bhatia, C.C. Jao, J.E. Rasmussen, S.L. Pedersen, K.J. Jensen, R. Langen, D. Stamou, Membrane curvature sensing by amphipathic helices: a single liposome study using alpha-synuclein and annexin B12, J. Biol. Chem. 286 (2011) 42603–42614.
[51] F. Forouhar, W.N. Huang, J.H. Liu, K.Y. Chien, W.G. Wu, C.D. Hsiao, Structural basis of membrane-induced cardiotoxin A3 oligomerization, J. Biol. Chem. 278 (2003) 21980–21988.
[52] S.C. Sue, P.K. Rajan, T.S. Chen, C.H. Hsieh, W. Wu, Action of Taiwan cobra cardiotoxin on membranes: binding modes of a beta-sheet polypeptide with phosphatidylcholine bilayers, Biochemistry 36 (1997) 9826–9836.
[53] A.G. Konshina, I.A. Boldyrev, Y.N. Utkin, A.V. Omel'kov, R.G. Efremov, Snake cytotoxins bind to membranes via interactions with phosphatidylserine head groups of lipids, PLoS One 6 (2011) e19064.
[54] W. Curatolo, B. Sears, L.J. Neuringer, A calorimetry and deuterium NMR study of mixed model membranes of 1-palmitoyl-2-oleylphosphatidylcholine and saturated phosphatidylcholines, Biochim. Biophys. Acta 817 (1985) 261–270.